

Efficient Long-Horizon GUI Agents via Training-Free KV Cache Compression

Bowen Zhou
Tsinghua University
Shenzhen, China
zhoubw25@mails.tsinghua.edu.cn

Zhou Xu
Tsinghua University
Shenzhen, China
xu-z25@mails.tsinghua.edu.cn

Wanli Li
Zhejiang University
Hangzhou, China
12521140@zju.edu.cn

Jingyu Xiao
The Chinese University of Hong Kong
Hong Kong, China
jyxiao@link.cuhk.edu.hk

Haoqian Wang*
Tsinghua University
Shenzhen, China
wangyizhai@sz.tsinghua.edu.cn

Abstract

Large Vision-Language Models (VLMs) have emerged as powerful engines for autonomous GUI agents, yet their deployment is severely constrained by the substantial memory footprint and latency of the Key-Value (KV) cache during long-horizon interactions. While existing cache compression methods have proven effective for LLMs, we empirically demonstrate that they suffer from suboptimal performance in GUI scenarios due to a fundamental misalignment: unlike general visual tasks where attention sparsity varies across layers, GUI attention patterns exhibit **uniform high-sparsity** across all transformer layers. Motivated by this insight, we propose **ST-Lite**, a training-free KV cache compression framework tailored for efficient GUI agents that explicitly addresses the dynamic spatio-trajectory dependencies within GUI data streams. ST-Lite introduces a novel dual-branch scoring policy incorporating **Component-centric Spatial Saliency (CSS)** and **Trajectory-aware Semantic Gating (TSG)**. Specifically, CSS preserves the structural integrity of interactive UI elements by evaluating local neighborhood saliency, while TSG mitigates historical redundancy by dynamically filtering visually repetitive KV pairs within the interaction trajectory. Extensive evaluations demonstrate that with only a 10-20% cache budget, ST-Lite achieves **2.45× decoding acceleration** while maintaining comparable or even superior performance compared to full-cache baselines, offering a scalable solution for resource-constrained GUI agents.

CCS Concepts

• **Computing methodologies** → **Artificial intelligence**.

Keywords

KV Cache, GUI Agents, Vision-Language Models, Efficiency

*Corresponding author.

Permission to make digital or hard copies of all or part of this work for personal or classroom use is granted without fee provided that copies are not made or distributed for profit or commercial advantage and that copies bear this notice and the full citation on the first page. Copyrights for components of this work owned by others than the author(s) must be honored. Abstracting with credit is permitted. To copy otherwise, or republish, to post on servers or to redistribute to lists, requires prior specific permission and/or a fee. Request permissions from permissions@acm.org.

Conference acronym 'XX, Woodstock, NY

© 2018 Copyright held by the owner/author(s). Publication rights licensed to ACM.

ACM ISBN 978-1-4503-XXXX-X/2018/06

<https://doi.org/XXXXXXXX.XXXXXXX>

ACM Reference Format:

Bowen Zhou, Zhou Xu, Wanli Li, Jingyu Xiao, and Haoqian Wang. 2018. Efficient Long-Horizon GUI Agents via Training-Free KV Cache Compression. In *Proceedings of Make sure to enter the correct conference title from your rights confirmation email (Conference acronym 'XX)*. ACM, New York, NY, USA, 15 pages. <https://doi.org/XXXXXXXX.XXXXXXX>

1 Introduction

The rise of Vision-Language Models (VLMs) has catalyzed the rapid development of autonomous Graphical User Interface (GUI) agents, enabling them to navigate complex digital environments and execute multi-step automated workflows [3, 6, 13, 19–21, 33, 39]. Despite demonstrating exceptional reasoning capabilities, GUI agents face a severe bottleneck: the substantial memory constraints and latency of the Key-Value (KV) cache during long-horizon interactions. Since GUI tasks typically involve high-resolution screenshots and extended interaction trajectories, the size of the KV cache grows linearly with sequence length, leading to severe GPU memory saturation and inference latency. This restricts their real-time interactive deployment on consumer-grade hardware.

To mitigate this challenge, researchers have explored training-free KV cache compression techniques. Initial breakthroughs in Large Language Models (LLMs), such as SnapKV [12] and PyramidKV [2], are primarily grounded in the **attention sink** or **hierarchical saliency** phenomena. While effective for text, these methods struggle to generalize to the multimodal domain. More recent VLM-specific strategies like VL-Cache [28] attempt to bridge this gap by introducing depth-based hierarchical allocation. However, our systematic analysis reveals a fundamental misalignment between these general-purpose strategies and the unique characteristics of GUI-VLM interactions.

Unlike general visual tasks, GUI screenshots possess discrete structured features, where functional elements are sparsely distributed over uniform backgrounds. We observe that GUI workloads exhibit a **uniform high-sparsity pattern** across all transformer layers, as illustrated in Figure 3, which directly contradicts the layer-wise budget assumptions of VL-Cache, leading to severe semantic loss. Furthermore, we demonstrate that window-based greedy selection mechanisms inherited from LLMs (e.g., SnapKV) tend to fall into local optimality traps when handling long-horizon tasks. By relying solely on local observation windows, such mechanisms fail

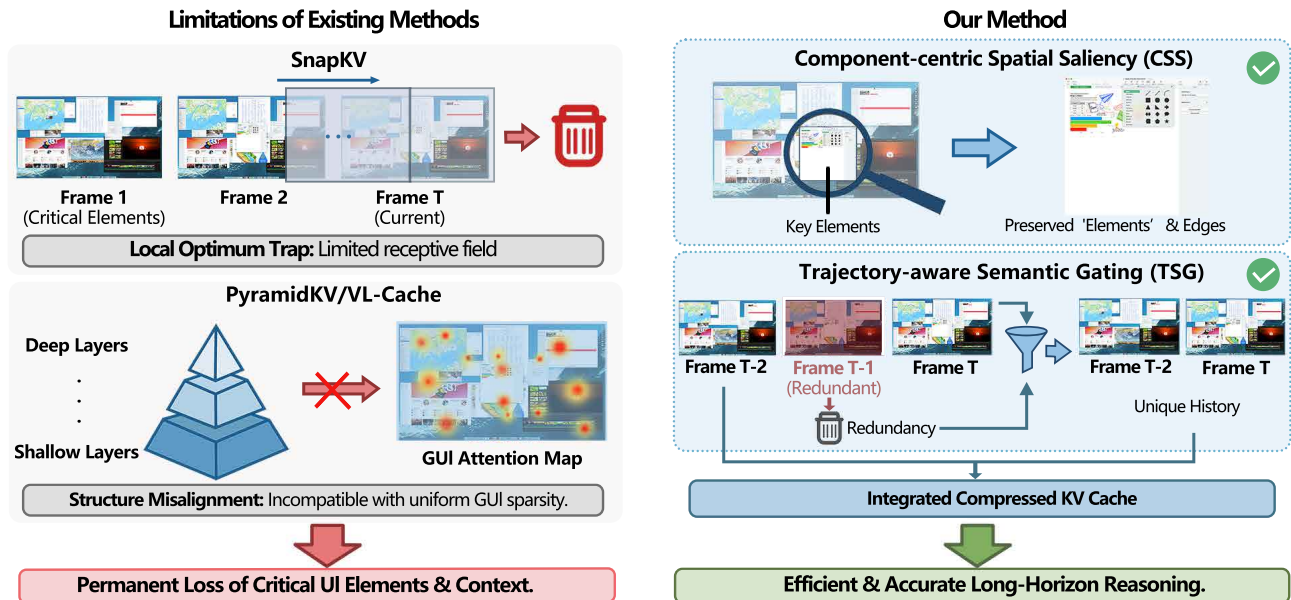


Figure 1: Conceptual illustration of ST-Lite compared with existing methods. The left side depicts the limitations of current strategies: window-based greedy methods (e.g., SnapKV) suffer from local optimum traps, while hierarchical allocation methods (e.g., PyramidKV) lead to structure misalignment. The right side demonstrates our ST-Lite, which integrates Component-centric Spatial Saliency (CSS) to preserve key interactive elements and Trajectory-aware Semantic Gating (TSG) to eliminate history redundancy, achieving efficient and accurate long-horizon reasoning.

to capture global spatio-trajectory dependencies, resulting in the irreversible loss of critical UI element information.

Addressing these challenges, we propose **ST-Lite** (Spatio-Trajectory Lite), a training-free KV cache compression framework tailored for efficient GUI agents, as illustrated in Figure 1. ST-Lite treats GUI interaction flows as long-horizon spatio-trajectory streams characterized by inherent high sparsity, and resolves the limitations of existing methods by explicitly mining local spatial distinctiveness and trajectory-aware semantic evolution. The framework consists of two core components: (1) **Component-centric Spatial Saliency (CSS)**: maintains the structural integrity of interactive GUI elements (e.g., buttons, icons) by identifying tokens with high relative saliency within their local neighborhood. This mechanism imposes a spatial inductive bias that preserves the high-frequency structural boundaries of functional components. (2) **Trajectory-aware Semantic Gating (TSG)**: ensures the cache stores only the unique history required for long-horizon reasoning by dynamically filtering visually repetitive KV pairs and mitigating semantic drift. TSG effectively distills the interaction trajectory into a sequence of critical state transitions.

To validate our approach, we conduct extensive evaluations across diverse GUI benchmarks, including ScreenSpot Pro [10], AITW [23], and AgentNetBench [32]. The results demonstrate that ST-Lite significantly enhances the efficiency of GUI agents without compromising capability. Specifically, operating within a constrained **10-20% cache budget**, our framework achieves a **2.45×**

decoding acceleration and outperforms state-of-the-art baselines by an average of **7.3%** in success rate across all benchmarks. Furthermore, our analysis reveals that active context simplification effectively mitigates semantic noise, enabling ST-Lite to **surpass even full-cache performance** on long-horizon tasks (AITW and AgentNetBench), offering a robust solution for resource-limited deployments.

Our primary contributions are summarized as follows:

- 1. Systematic Diagnostic Analysis.** We provide a rigorous analysis of existing training-free compression methods in GUI contexts. We identify a fundamental misalignment between hierarchical budget allocation and the uniform attention patterns inherent to GUIs, while demonstrating how greedy window mechanisms fall into local optima during long-horizon interactions.
- 2. ST-Lite Framework.** We introduce a novel spatio-trajectory KV cache compression framework grounded in context-aware simplification. By leveraging Component-centric Spatial Saliency (CSS) and Trajectory-aware Semantic Gating (TSG), ST-Lite preserves structural integrity and filters stationary redundancies without requiring auxiliary training.
- 3. Empirical Validation.** Extensive evaluations across multiple benchmarks demonstrate that ST-Lite achieves a superior trade-off between efficiency and performance, enabling high-performance GUI agents to operate effectively on hardware with limited memory capacity.

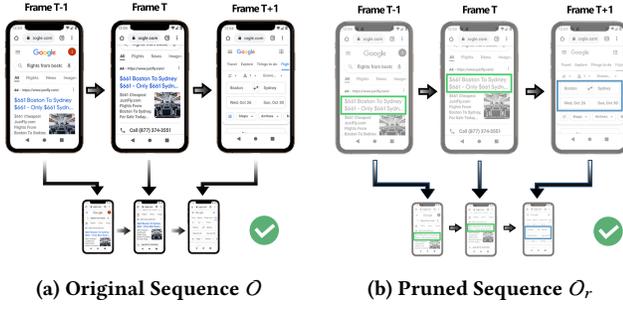


Figure 2: Comparison of task execution flows under different context settings. (a) The original interaction sequence O containing full historical frames leads to successful task completion. (b) The pruned sequence O_r , despite removing trajectory-wise redundant frames, also results in success. This visual evidence confirms that high historical redundancy exists in GUI tasks and that our aggressive compression preserves the essential semantic cues required for correct agent decision-making.

2 Related Work

2.1 Efficient GUI Agents

GUI agents represent a specialized domain within Vision-Language Models (VLMs), tasked with processing continuous streams of screenshots to automate complex workflows. Unlike natural images, GUI screenshots possess unique discrete structural characteristics. **ShowUI** [16] conceptualizes GUI interfaces as graph structures composed of discrete functional components, while **Ferret-UI** [38] emphasizes the necessity of preserving local sub-image details for precise element grounding.

However, this high density of visual context inevitably introduces substantial redundancy [25, 26, 26, 27], which has recently drawn increasing attention from the research community [5, 8, 9, 14, 15, 17, 24, 37, 40]. As analyzed in **SimpAgent** [4], GUI data is characterized by **high-density but loose-relation** noise, where functionally irrelevant static backgrounds consume significant processing resources. In the trajectory dimension, long-horizon tasks exacerbate this issue. **OS-Atlas**'s [34] large-scale analysis reveals extremely high inter-frame similarity in GUI operation streams, and **Mobile-Agent-v2** [29] demonstrates that blindly retaining full history leads to context loss and hallucination. Consequently, the accumulation of massive, highly redundant visual tokens in the KV cache has become a critical bottleneck, restricting the deployment of GUI agents in real-time, long-context scenarios.

2.2 KV Cache Compression in LLMs and VLMs

To alleviate memory overhead in long-context inference, researchers have developed various training-free KV cache compression strategies [35, 41]. In the realm of LLMs, SnapKV [12] introduces a fine-tuning-free method that identifies key tokens using a local observation window at the end of the prompt. PyramidKV [2] leverages the pyramidal information funneling phenomenon, allocating more cache budget to shallow layers where attention is broader. Similarly,

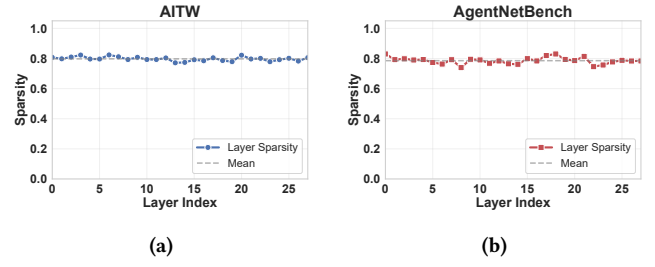


Figure 3: Layer-wise Attention Sparsity Analysis. Unlike the hierarchical sparsity variation observed in LLMs and general vision models, GUI agents exhibit a uniform high-sparsity pattern across all transformer layers on both (a) AITW and (b) AgentNetBench datasets. This justifies our uniform budget allocation strategy.

L2 Norm-Based strategies [7] utilize the magnitude of Key embeddings as a proxy for attention importance. Moving to multi-modal models, VL-Cache [28] pioneered modality-aware compression, proposing a layer-adaptive budget allocation mechanism based on the distinct contribution patterns of visual and text tokens.

Despite their effectiveness in general domains, these methods are ill-suited for GUI scenarios. General visual strategies fail to account for the uniform high-sparsity of GUI elements across layers, leading to structural misalignment. Furthermore, window-based greedy approaches, represented by SnapKV, often get trapped in local optima in long-horizon GUI streams, discarding critical historical elements that receive negligible attention from the observation window. To address these limitations, we explicitly align cache retention with the inherent structural layout of UI components and the sequential dependencies of interaction history. This spatio-trajectory guidance strategy effectively filters redundancy while preserving the precise context required for autonomous decision-making.

3 Preliminary

3.1 Problem Definition

We formulate GUI navigation as a **Long-Horizon Autoregressive Generation** task. Let π_θ denote a VLM agent. At time step t , given a user instruction I and a high-resolution screenshot $o_t \in \Omega$ [18], the agent generates an action $a_t \in \mathcal{A}$ conditioned on the cumulative history H_t [31]. We define the history context as the sequence of all past observations and actions:

$$H_t = \{(o_0, a_0), (o_1, a_1), \dots, (o_{t-1}, a_{t-1})\}. \quad (1)$$

The inference objective is to maximize the likelihood of the optimal action:

$$a_t = \operatorname{argmax}_{a \in \mathcal{A}} P(a \mid I, o_t, H_t; \theta). \quad (2)$$

However, strictly adhering to Eq. (2) imposes a severe computational burden due to the **Visual Token Explosion** inherent in high-resolution GUI streams. Consequently, our objective is to construct a cache compression mapping that minimizes the memory footprint of H_t while preserving the essential spatio-trajectory context required for accurate decision-making.

3.2 KV Cache Compression Formulation

Efficient inference in Vision-Language Models relies heavily on the Key-Value (KV) cache mechanism to avoid redundant computations. This process typically unfolds in two phases [28]: the **Prefill Phase**, where multimodal inputs (screenshots and instructions) are encoded in parallel to generate the initial KV states; and the **Decoding Phase**, where the model auto-regressively generates action tokens. During decoding, the KV cache grows linearly with the interaction steps. For GUI agents maintaining long-horizon history H_t , this results in substantial **memory bottlenecks and inference latency**.

Formally, let $K^{(l)}, V^{(l)} \in \mathbb{R}^{L \times D}$ denote the cached Key and Value matrices at layer l for a sequence of length L . The objective of cache compression is to derive a compressed subset of indices \mathcal{I}_{keep} with size $B \ll L$, such that the approximation error of the attention output is minimized. Existing compression paradigms primarily optimize this through two dimensions:

Budget Allocation. While standard approaches often adopt a uniform strategy that distributes memory budgets equally across all layers [12, 35, 41], advanced methods acknowledge that different transformer layers exhibit varying sensitivities to information loss. Consequently, they often employ hierarchical decay schedules [2, 28], assigning larger cache budgets to shallower layers (which capture broad visual semantics) and smaller budgets to deeper layers. However, this assumes a hierarchical feature evolution that may not hold for the discrete, high-density elements found in GUI screenshots.

Token Scoring Policy. Given a layer-specific budget, a scoring function $A : \{1, \dots, L\} \rightarrow \mathbb{R}$ is required to rank the importance of each historical token. We construct our **fundamental scoring mechanism** using the voting strategy from SnapKV [12], which we formally term the **Base Attention Prior** (A_{base}). This metric estimates the intrinsic importance of a token by accumulating the attention weights it receives from the most recent observation window (the last δ tokens):

$$A_{base}^{(i)} = \sum_{q=L-\delta+1}^L \text{Attn}(q, i) = \sum_{q=L-\delta+1}^L \text{Softmax}\left(\frac{\mathbf{q}_q \cdot \mathbf{k}_i^\top}{\sqrt{d}}\right). \quad (3)$$

where $\mathbf{q}_q, \mathbf{k}_i \in \mathbb{R}^D$ represent the query and key vectors, and d denotes the head dimension. The final selection policy is governed by the Top- B operator:

$$\mathcal{I}_{keep} = \text{Top}_B\left(\{A_{base}^{(i)}\}_{i=1}^L\right). \quad (4)$$

where $A_{base}^{(i)}$ represents the final score (to be refined in subsequent sections). We define the target budget B based on a compression ratio $\beta \in (0, 1]$ such that $B = \lfloor \beta \cdot L \rfloor$.

3.3 Diagnostic Analysis

We conducted a diagnostic evaluation of representative methods—SnapKV (window-based) and PyramidKV (hierarchical allocation)—on GUI benchmarks. As shown in Figure 5, these methods suffer from performance plateaus. We mathematically formalize the root causes of these failures to motivate our approach.

Failure Mode 1: The Local Optimality Trap. To rigorously explain the failure of window-based methods, we analyze the interplay between Recency Bias and the Softmax mechanism. Let $s_{q,k}$ denote the raw attention score. Extensive studies [35, 41] establish that due to positional encoding biases, current queries assign significantly higher scores to immediate neighbors $j \in \mathcal{W}_{obs}$ than to distant critical tokens i^* , creating an empirical semantic gap $\Delta = s_{q,j} - s_{q,i^*} > 0$. The Softmax function exponentially amplifies this linear gap:

$$\begin{aligned} \text{Attn}(q, i^*) &= \frac{e^{s_{q,i^*}}}{e^{s_{q,i^*}} + \sum_{k \neq i^*} e^{s_{q,k}}} \\ &\leq \frac{e^{s_{q,i^*}}}{e^{s_{q,i^*}} + e^{s_{q,j}}} = \frac{1}{1 + e^\Delta}. \end{aligned} \quad (5)$$

As Δ increases, the term e^Δ dominates the denominator, driving the probability mass $\text{Attn}(q, i^*)$ rapidly toward zero. Consequently, the accumulated score $A_{base}(i^*) \approx 0$, mathematically guaranteeing that distant global anchors are ranked lower than local noise and permanently evicted.

Failure Mode 2: Incompatibility of Hierarchical Allocation. PyramidKV assumes attention sparsity converges pyramidally with depth. However, GUI interfaces consist of discrete, semantically independent components (Icons, Buttons) that require consistent maintenance across all transformer layers to preserve functional semantics. By probing UI-TARS-1.5-7B on AITW [23] and Agent-NetBench [32], we observe a distinct **Uniform Sparsity** pattern (Figure 3):

$$|\nabla_l \mathcal{S}^{(l)}| < \epsilon, \quad \forall l \in [1, L_{max}]. \quad (6)$$

Existing hierarchical methods calculate layer-wise budgets via normalization: $B^{(l)} = \text{Norm}\left(\sum \text{Attn}^{(l)}\right) \cdot B_{total}$. When sparsity differences across layers are negligible ($|\nabla_l \mathcal{S}^{(l)}| \approx 0$), this normalization mechanism artificially amplifies random numerical noise, resulting in a chaotic budget distribution that fundamentally misaligns with the structured, layer-agnostic nature of GUI representations.

Design Insight. These findings compel us to seek a strategy that adopts uniform allocation across layers while explicitly mining **Long-horizon spatio-trajectory dependencies**.

4 ST-Lite Framework

Addressing the aforementioned misalignments, we propose **ST-Lite** (Spatio-Trajectory Lite), a training-free KV Cache compression framework, as illustrated in Figure 4. We introduce two core components: **Component-centric Spatial Saliency (CSS)** for maintaining spatial structural integrity, and **Trajectory-aware Semantic Gating (TSG)** for eliminating historical redundancy.

4.1 Component-centric Spatial Saliency (CSS)

Unlike natural images with smooth texture variations, GUI interfaces consist of discrete functional elements superimposed on uniform backgrounds. Information is sparse and concentrated at *boundaries*. We propose the **Component-centric Spatial Saliency (CSS)** mechanism to identify this local spatial distinctiveness.

Intrinsic Structural Unit. We argue that in a discrete rasterized grid, the definition of neighborhood should reflect the local

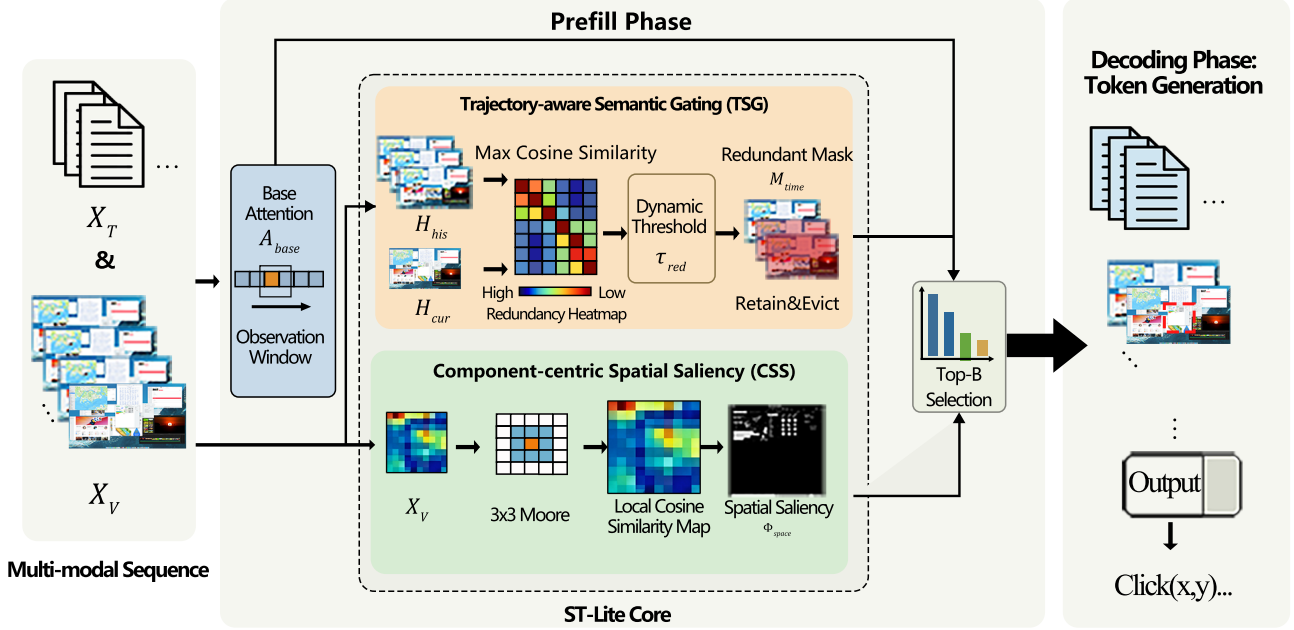


Figure 4: The overall architecture of ST-Lite. Our framework dynamically optimizes the KV cache through two synergistic modules: (1) Component-centric Spatial Saliency (CSS), which identifies and preserves spatially salient regions (e.g., functional buttons) within each frame using attention heatmap analysis; and (2) Trajectory-aware Semantic Gating (TSG), which filters out redundant historical states by measuring semantic shifts between consecutive frames. By integrating these spatial and historical policies, ST-Lite effectively reduces memory footprint while maintaining high precision in long-horizon GUI tasks.

manifold structure. We utilize the Moore Neighborhood (the central cell and its 8 neighbors), forming a fixed 3×3 kernel. This zero-hyperparameter design efficiently mines local structural consistency without training overhead.

Mechanism Principle. We measure the *relative uniqueness* of a Token within its local manifold. Let $h_{u,v} \in \mathbb{R}^D$ be the hidden state of the visual token at grid coordinate (u, v) . We first define a **Local Uniformity Score** $\mathcal{H}_{u,v}$ by computing the average cosine similarity between the central token and its neighbors:

$$\begin{aligned} \mathcal{H}_{u,v} &= \frac{1}{|\mathcal{N}_{u,v}|} \sum_{(p,q) \in \mathcal{N}_{u,v}} \text{Cos}(h_{u,v}, h_{p,q}) \\ &= \frac{1}{8} \sum_{(p,q) \in \mathcal{N}_{u,v}} \frac{h_{u,v} \cdot h_{p,q}}{\|h_{u,v}\| \|h_{p,q}\|}. \end{aligned} \quad (7)$$

where $\mathcal{N}_{u,v}$ represents the 8 spatial neighbors within the 3×3 grid. A high $\mathcal{H}_{u,v}$ indicates the token belongs to a uniform background, carrying minimal structural information. Conversely, a low $\mathcal{H}_{u,v}$ implies the existence of semantic boundaries. Therefore, we define the **Spatial Saliency Score** Φ_{space} as the complement of uniformity:

$$\Phi_{space}(x_i) = 1 - \mathcal{H}_{u,v}. \quad (8)$$

where x_i denotes the KV pair corresponding to the visual token at spatial coordinate (u, v) . By prioritizing tokens with high local distinctiveness, CSS effectively suppresses redundant background

pixels while preserving the skeleton of the GUI—buttons, text, and icons.

4.2 Trajectory-aware Semantic Gating (TSG)

GUI workflows exhibit high historical redundancy and **semantic context shifts**. We introduce a similarity-based eviction strategy to filter historical tokens that are semantically identical to the current view.

Let H_{his} and H_{cur} be the hidden states of historical frames and the current frame, respectively. For each historical token h_i , we calculate its redundancy score ρ_i as its maximum cosine similarity with the current frame:

$$\rho_i = \max_{h_j \in H_{curr}} \cos(h_i, h_j) = \max_{h_j \in H_{curr}} \left(\frac{h_i \cdot h_j}{\|h_i\| \|h_j\|} \right). \quad (9)$$

To determine the eviction gate, we establish a dynamic redundancy threshold τ_{red} constrained by a target budget B . Let $\hat{\rho}$ denote the sequence of redundancy scores sorted in **ascending order** (i.e., from most unique to most redundant). The dynamic threshold is defined as the score at the rank corresponding to the budget B :

$$\tau_{red} = \hat{\rho}_B, \quad \text{where } \hat{\rho} = \text{Sort}_{\text{asc}}(\{\rho_i\}). \quad (10)$$

This formulation ensures that the threshold adaptively shifts based on the distribution of semantic similarity, retaining the B tokens with the lowest redundancy. The semantic gate $M_{time}^{(i)}$ is

then formalized as:

$$M_{time}^{(i)} = \begin{cases} 0 \text{ (Evict)}, & \text{if } \rho_i > \tau_{red} \\ 1 \text{ (Retain)}, & \text{if } \rho_i \leq \tau_{red} \end{cases}. \quad (11)$$

By filtering out tokens where ρ_i is above the threshold, ST-Lite forces the KV Cache to store only the *unique* history required for reasoning.

4.3 Integrated KV Eviction Policy

To synthesize insights from both spatial and historical dimensions, ST-Lite adopts a modality-aware scoring mechanism. For the i -th Token, its final retention score $\mathcal{S}^{(i)}$ is defined as follows:

$$\mathcal{S}^{(i)} = \begin{cases} A_{base}^{(i)}, & \text{if } x_i \in X_T \\ M_{time}^{(i)} \cdot (A_{base}^{(i)} + \Phi_{space}(x_i)), & \text{if } x_i \in X_V \end{cases}. \quad (12)$$

The physical meaning of each term is as follows:

- $A_{base}^{(i)}$ is the **Base Attention Prior** calculated based on the observation window, capturing global semantic relevance;
- $\Phi_{space}(x_i)$ represents the **Spatial Structure Enhancement Score**, derived from Component-centric Spatial Saliency (CSS);
- $M_{time}^{(i)} \in \{0, 1\}$ is the **Hard Gate** generated by Trajectory-aware Semantic Gating (TSG), which serves as a first-order filter to prune historical redundancy before spatial scoring is applied.

Finally, the system selects the Top- B tokens with the highest scores to construct the compressed KV Cache [12, 35, 41].

5 Experiment

This section verifies the effectiveness of **ST-Lite** through quantitative evaluation and qualitative analysis, focusing on: (1) ST-Lite’s performance retention capability compared to existing compression algorithms under low-to-medium cache budgets (10%–40%); (2) the specific contributions of **Component-centric Spatial Saliency (CSS)** and **Trajectory-aware Semantic Gating (TSG)** to context simplification.

5.1 Experimental Setup

Benchmarks. To comprehensively assess the efficacy of ST-Lite across varying levels of interaction complexity, we conducted evaluations on seven representative GUI benchmarks, with our primary analysis centering on three distinct scenarios: ScreenSpot Pro [10], which rigorously tests precise element localization in single-frame high-resolution environments; AITW (Android in the Wild) [23], which evaluates historical reasoning capabilities essential for multi-step, long-horizon interactions; and AgentNet-Bench [32], which assesses the comprehensive decision-making performance of Web agents in complex workflows. Full experimental results for additional benchmarks, specifically ScreenSpotV2 [34], OSWorld-Verified [36], Multimodal-Mind2Web [42], and Android-Control [11], are provided in Appendix D to demonstrate generalization.

Baselines and Implementation. To verify the model-agnostic effectiveness of ST-Lite, we deployed it on two representative GUI agent backbones with distinct architectures and training paradigms: UI-TARS-1.5-7B [22], which is built upon the Qwen2.5-VL [1] architecture and aligned via Supervised Fine-Tuning (SFT) combined

with Reinforcement Learning from Human Feedback (RLHF); and OpenCUA-7B [32], which utilizes Qwen2-VL [30] as its base and is trained exclusively via SFT. Our method is benchmarked against three leading training-free compression strategies: SnapKV [12], which employs a heuristic eviction policy based on local observation windows; PyramidKV [2], which utilizes a hierarchical differentiated budget allocation strategy; and VL-Cache [28], a modality-aware hierarchical allocation method. Furthermore, to isolate the specific contributions of our proposed modules, we introduced ablation variants **ST-Lite (CSS Only)** and **ST-Lite (TSG Only)**, thereby decoupling the gains from spatial structural preservation and historical redundancy filtering. For comprehensive details regarding experimental configurations, dataset statistics, and hyperparameter settings, please refer to **Appendix A and Appendix B**.

5.2 Main Results

We evaluate the performance of **ST-Lite** by sweeping the KV cache budget ratio β from 1% to 100%. The results, summarized in Figure 5 and Table 4, demonstrate that our method consistently establishes a superior trade-off between inference performance and efficiency across all benchmarks.

Superior Robustness under Extreme Budgets. Under highly constrained memory settings ($\beta \in [10\%, 40\%]$), ST-Lite exhibits significant performance resilience compared to baselines. Notably, on the ScreenSpot Pro single-frame high-resolution benchmark, hierarchical allocation strategies such as PyramidKV and VL-Cache experience catastrophic performance decay as the budget decreases. This collapse stems from their inherent assumption of hierarchical attention concentration, which is fundamentally misaligned with the discrete, uniformly sparse nature of GUI screenshots. In contrast, by explicitly identifying structural boundaries through the Component-centric Spatial Saliency (CSS) module, ST-Lite preserves critical UI elements (e.g., small icons and buttons) even at extreme compression ratios, maintaining an accuracy trajectory that closely tracks the full-cache performance.

Noise Suppression and Less-is-More [4] Phenomenon. In long-horizon interaction tasks such as AITW and AgentNetBench, ST-Lite reveals a compelling observation: context simplification can lead to better-than-full-cache performance. Specifically, at a 20% budget on AITW, ST-Lite achieves a **20.7%** success rate, surpassing the **18.7%** of the Full Cache. We hypothesize that for GUI agents, historical trajectories are often contextually dynamic and filled with visually repetitive but semantically redundant state transitions. By employing **Trajectory-aware Semantic Gating (TSG)**, ST-Lite acts as a dynamic information filter that prunes these stale KV pairs. This process effectively mitigates the **Context Poisoning** effect, where accumulated irrelevant history introduces noise that distracts the model from current goal-directed reasoning.

Crucially, we observe a distinct pattern in cross-model robustness: UI-TARS-1.5-7B exhibits significantly higher tolerance to aggressive compression compared to OpenCUA-7B. For instance, at a **10%** budget on AITW, UI-TARS equipped with ST-Lite achieves an **18.4%** success rate, which not only approaches but slightly surpasses the **18.2%** performance of the Full Cache baseline. This **Less-is-More** phenomenon suggests that ST-Lite effectively filters out semantic noise in long-horizon trajectories, whereas OpenCUA,

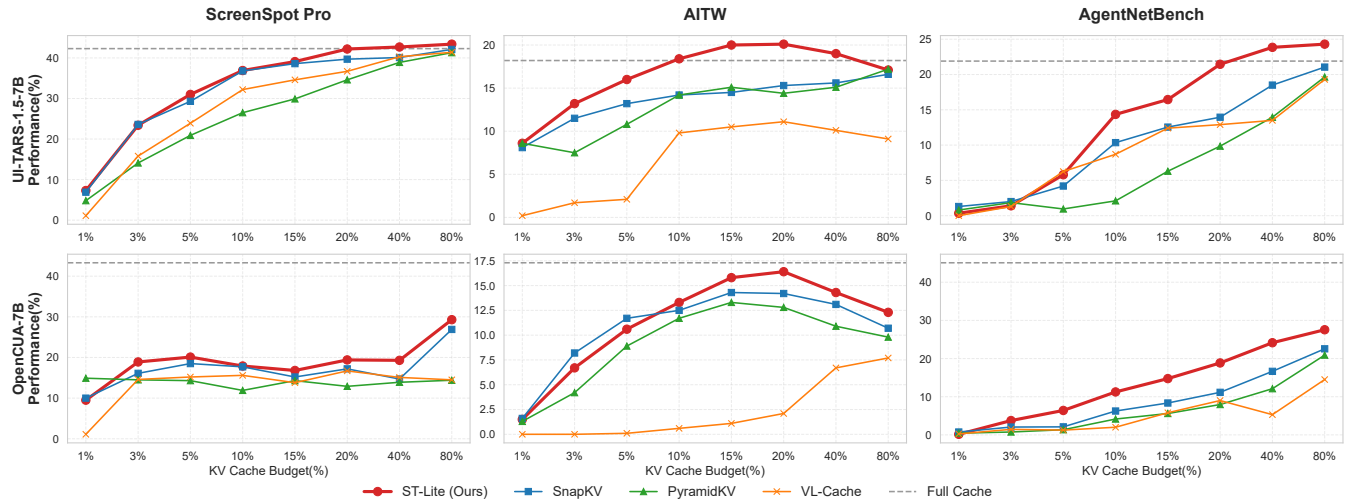


Figure 5: Evaluation results on ScreenSpot Pro, AITW, and AgentNetBench with varied cache budgets. ST-Lite achieves comparable accuracy against Full Cache and outperforms multiple baselines with limited KV cache budget. Interestingly, we found that ST-Lite occasionally performs slightly better with a partial KV cache (e.g., on AITW). We attribute it to the regularization effect of KV cache compression.

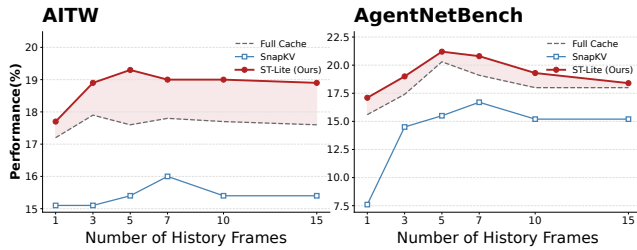


Figure 6: Impact of historical frame count on model success rate. As context length increases, baseline methods suffer performance decay due to noise accumulation, while ST-Lite demonstrates stable performance gains.

while benefiting from ST-Lite, still finds it challenging to match its full-cache ceiling.

We attribute this performance divergence to the combined effects of **architectural evolution and training paradigms**. Structurally, UI-TARS benefits from the advanced attention mechanisms of its Qwen2.5-VL backbone, which represents a generation leap over OpenCUA’s Qwen2-VL foundation. More importantly, unlike OpenCUA which relies exclusively on Supervised Fine-Tuning (SFT), UI-TARS incorporates Reinforcement Learning from Human Feedback (RLHF) [22]. This RL alignment process implicitly acts as a regularizer, encouraging the model to learn sparse, high-utility feature representations that are intrinsically more robust to token eviction. Despite these disparities, it is noteworthy that ST-Lite consistently outperforms all three state-of-the-art baselines (SnapKV, PyramidKV, and VL-Cache) across both UI-TARS and OpenCUA architectures. This universality confirms that the spatio-trajectory redundancy targeted by CSS and TSG is an intrinsic property of

GUI-VLM interactions, independent of the specific model capacity or training methodology.

5.3 Ablation Study

To decouple the contributions of the spatial and historical dimensions, Table 1 presents the performance of each component at a 20% budget. We further investigate the framework’s scalability relative to historical trajectory length in Figure 6.

Table 1: Ablation Analysis: Performance contributions of Component-centric Spatial Saliency (CSS) and Trajectory-aware Semantic Gating (TSG) at a 20% budget.

Method	ScreenSpot (Acc.)	AITW (Acc.)	AgentNet (Acc.)
Full Cache	42.3	18.7	17.5
SnapKV	39.7	8.0	19.0
ST-Lite (CSS only)	40.2	14.1	18.7
ST-Lite (TSG only)	39.6	18.9	19.5
ST-Lite	40.2	20.7	20.5

Efficacy of Spatial Saliency (CSS). As shown in Table 1, **ST-Lite (CSS only)** yields the most significant improvements on the ScreenSpot Pro benchmark compared to the SnapKV baseline. By explicitly evaluating local neighborhood contrast, CSS effectively discriminates functional UI components from uniform background noise. This ensures that even when 80% of the cache is evicted, the structural skeleton required for precise element grounding remains intact, thereby maintaining a high grounding accuracy (40.2%).

Efficacy of Semantic Gating (TSG). We evaluate **ST-Lite (TSG only)** to assess the impact of historical filtering. TSG demonstrates its strength in long-horizon tasks such as AITW and AgentNetBench. Notably, on AgentNetBench, TSG alone (19.5%) outperforms

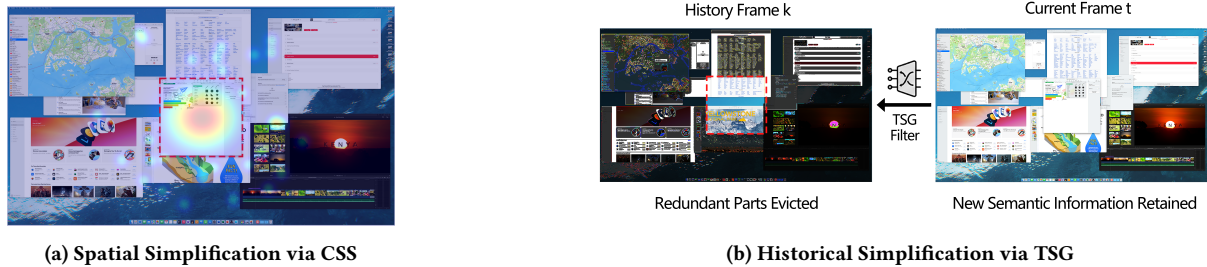


Figure 7: Qualitative visualization of ST-Lite. The red bounding boxes indicate the actual regions requiring attention (Ground Truth). (a) The heatmap shows that CSS precisely targets these structural boundaries (e.g., buttons). (b) The black regions represent the redundant historical parts evicted by TSG. This demonstrates that ST-Lite effectively preserves critical information within the red boxes while discarding redundancy.

the CSS-only variant, confirming that mitigating historical redundancy is the primary bottleneck for complex workflows. By discarding visually repetitive KV pairs, TSG prevents the model from being overwhelmed by stale information.

Spatio-Trajectory Synergy. The full ST-Lite framework achieves the highest performance across all benchmarks, particularly on AITW, where it outperforms individual components by a substantial margin. This synergy suggests that retaining spatial structural elements (via CSS) while simultaneously updating the trajectory with semantic novelty (via TSG) is essential for robust GUI navigation.

Scalability and History Length. As illustrated in Figure 6, baseline methods suffer from performance decay beyond a 7-frame threshold due to **Context Poisoning**, where accumulated historical noise distracts the model. In contrast, ST-Lite demonstrates superior scalability; by leveraging TSG to filter stationary redundancies, it maintains a positive performance trajectory even as the history length extends to 10 frames or more, effectively decoupling inference robustness from sequence length.

5.4 Efficiency and Scalability Analysis

We conducted efficiency profiling on selected long-horizon tasks from AgentNetBench (specifically samples exceeding 15 frames) to evaluate system performance under heavy loads. As detailed in Table 2, ST-Lite demonstrates superior scalability as the context length grows.

Table 2: Inference speedup across different screenshot scales. While the prefill phase incurs negligible overhead (speedup ≈ 1.0), ST-Lite significantly accelerates the memory-bound decoding phase (up to $2.45\times$), resulting in robust end-to-end efficiency.

Screenshots	Prefill Speedup	Decoding Speedup	End-to-End Speedup
3	0.98	1.25	1.15
5	0.99	1.68	1.33
10	0.99	2.45	1.40

Decoding Latency Breakthrough. Notably, with a 10-frame history trajectory, ST-Lite achieves a remarkable $2.45\times$ **decoding**

speedup. This confirms that our method effectively prunes redundant KV states, preventing memory bandwidth saturation during the autoregressive generation phase, which is critical for real-time interactivity.

Zero-overhead Integration. Crucially, the prefill speedup remains consistently near $1.0\times$ (0.98–0.99) across all scales. This indicates that the computational overhead introduced by computing CSS and TSG scores is negligible compared to the visual encoding process. Consequently, despite the fixed latency cost of the vision encoder, ST-Lite still yields a substantial $1.4\times$ **end-to-end system speedup**, offering a practical solution for deployment on consumer-grade hardware.

5.5 Qualitative Analysis

To validate the effectiveness of **ST-Lite**, we visualize the attention distribution and token retention patterns in Figure 7. A broader visual comparison against baseline methods is detailed in **Appendix F**.

Structural Element Preservation via CSS. As shown in Figure 7(a), our **Component-centric Spatial Saliency (CSS)** acts as a precise spatial filter. While baseline visualizations in Figure 8 frequently exhibit attentional drift where the retained focus is scattered or shifted away from the target center—our method tightly contours the boundaries of interactive elements. Specifically, heuristic methods often produce fragmented attention maps that fail to cover the full semantic extent of the widget, creating unintended blind spots within the clickable region. In contrast, ST-Lite maintains robust spatial anchors by ensuring the retained attention mass forms a coherent and dense coverage over the UI component. By avoiding the diffused activation patterns common in other methods, we ensure that fine-grained controls remain sharp and addressable for coordinate prediction.

Historical Denoising via TSG. Figure 7(b) demonstrates the efficacy of **Trajectory-aware Semantic Gating (TSG)** in handling temporal redundancy. In long-horizon interactions, standard retention strategies often fail to cleanly separate static backgrounds from active content, resulting in attention maps cluttered with stationary noise (see Figure 8). As evidenced by the comparison, conventional methods tend to preserve obsolete visual states, leading to cache pollution where the model’s focus is distracted by irrelevant historical background pixels. Conversely, our approach

successfully blacks out these redundant regions, as visualized by the clean, high-contrast attention masks. This proves that ST-Lite strictly allocates the limited cache budget to high-value semantic updates, preventing the agent’s reasoning from being diluted by the lingering visual artifacts observed in baseline outputs.

6 Conclusion

In this paper, we address the efficiency bottleneck of GUI agents with ST-Lite, a training-free KV cache compression framework designed for operation under strict KV cache budgets. By integrating Component-centric Spatial Saliency (CSS) and Trajectory-aware Semantic Gating (TSG), ST-Lite effectively identifies and preserves critical spatio-temporal anchors. Our extensive experiments demonstrate that ST-Lite significantly reduces KV cache memory footprint and enhances inference efficiency while maintaining task success rates comparable to full cache baselines on long-horizon benchmarks. Ultimately, by shifting the compression paradigm from passive retention to active, semantics-driven selection, ST-Lite paves the way for deploying scalable, autonomous agents in real-world environments where extended interaction capability is essential.

Acknowledgments

This work was supported by the [Funding Agency Name] under Grant No. [XXXXXX]. We thank the anonymous reviewers for their constructive comments.

References

- [1] Shuai Bai, Keqin Chen, Xuejing Liu, Jialin Wang, Wenbin Ge, Sibao Song, Kai Dang, Peng Wang, Shijie Wang, Jun Tang, et al. 2025. Qwen2.5-vl technical report. *arXiv preprint arXiv:2502.13923* (2025).
- [2] Zefan Cai, Yichi Zhang, Bofei Gao, Yuliang Liu, Yucheng Li, Tianyu Liu, Keming Lu, Wayne Xiong, Yue Dong, Junjie Hu, et al. 2024. Pyramidkv: Dynamic kv cache compression based on pyramidal information funneling. *arXiv preprint arXiv:2406.02069* (2024).
- [3] Hyungjoo Chae, Namyoun Kim, Kai Tzu-iunn Ong, Minju Gwak, Gwanwoo Song, Jihoon Kim, Sunghwan Kim, Dongha Lee, and Jinyoung Yeo. 2024. Web agents with world models: Learning and leveraging environment dynamics in web navigation. *arXiv preprint arXiv:2410.13232* (2024).
- [4] Gongwei Chen, Xurui Zhou, Rui Shao, Yibo Lyu, Kaiwen Zhou, Shuai Wang, Wentao Li, Yinchuan Li, Zhongang Qi, and Liqiang Nie. 2025. Less is more: Empowering gui agent with context-aware simplification. In *Proceedings of the IEEE/CVF International Conference on Computer Vision*. 5901–5911.
- [5] Liang Chen, Haozhe Zhao, Tianyu Liu, Shuai Bai, Junyang Lin, Chang Zhou, and Baobao Chang. 2024. An image is worth 1/2 tokens after layer 2: Plug-and-play inference acceleration for large vision-language models. In *European Conference on Computer Vision*. Springer, 19–35.
- [6] Filippos Christianos, Georgios Papoudakis, Matthieu Zimmer, Thomas Coste, Zhihao Wu, Jingxuan Chen, Khyati Khandelwal, James Doran, Xidong Feng, Jiacheng Liu, et al. 2023. Pangu-agent: A fine-tunable generalist agent with structured reasoning. *arXiv preprint arXiv:2312.14878* (2023).
- [7] Alessio Devoto, Yu Zhao, Simone Scardapane, and Pasquale Minervini. 2024. A Simple and Effective L_2 Norm-Based Strategy for KV Cache Compression. *arXiv preprint arXiv:2406.11430* (2024).
- [8] Wenbo Hu, Yifan Xu, Yi Li, Weiyue Li, Zeyuan Chen, and Zhuowen Tu. 2024. Bliva: A simple multimodal llm for better handling of text-rich visual questions. In *Proceedings of the AAAI Conference on Artificial Intelligence*, Vol. 38. 2256–2264.
- [9] Junnan Li, Dongxu Li, Silvio Savarese, and Steven Hoi. 2023. Blip-2: Bootstrapping language-image pre-training with frozen image encoders and large language models. In *International conference on machine learning*. PMLR, 19730–19742.
- [10] Kaixin Li, Ziyang Meng, Hongzhan Lin, Ziyang Luo, Yuchen Tian, Jing Ma, Zhiyong Huang, and Tat-Seng Chua. 2025. Screenspot-pro: Gui grounding for professional high-resolution computer use. In *Proceedings of the 33rd ACM International Conference on Multimedia*. 8778–8786.
- [11] Wei Li, William E Bishop, Alice Li, Christopher Rawles, Folawiyi Campbell-Ajala, Divya Tyamagundlu, and Oriana Riva. 2024. On the effects of data scale on ui control agents. *Advances in Neural Information Processing Systems* 37 (2024), 92130–92154.
- [12] Yuhong Li, Yingbing Huang, Bowen Yang, Bharat Venkitesh, Acyr Locatelli, Hanchen Ye, Tianle Cai, Patrick Lewis, and Deming Chen. 2024. SnapKV: LLM knows what you are looking for before generation. *Advances in Neural Information Processing Systems* 37 (2024), 22947–22970.
- [13] Yinchuan Li, Xinyu Shao, Jianping Zhang, Haozhi Wang, Leo Maxime Brunswic, Kaiwen Zhou, Jiqian Dong, Kaiyang Guo, Xiu Li, Zhitang Chen, et al. 2025. Generative models in decision making: A survey. *arXiv preprint arXiv:2502.17100* (2025).
- [14] Yanwei Li, Chengyao Wang, and Jiaya Jia. 2024. Llama-vid: An image is worth 2 tokens in large language models. In *European Conference on Computer Vision*. Springer, 323–340.
- [15] Yanwei Li, Yuechen Zhang, Chengyao Wang, Zhisheng Zhong, Yixin Chen, Ruihang Chu, Shaoteng Liu, and Jiaya Jia. 2025. Mini-gemini: Mining the potential of multi-modality vision language models. *IEEE Transactions on Pattern Analysis and Machine Intelligence* (2025).
- [16] Kevin Qinghong Lin, Linjie Li, Difei Gao, Zhengyuan Yang, Shiwei Wu, Zechen Bai, Stan Weixian Lei, Lijuan Wang, and Mike Zheng Shou. 2025. Showui: One vision-language-action model for gui visual agent. In *Proceedings of the Computer Vision and Pattern Recognition Conference*. 19498–19508.
- [17] Yuliang Liu, Biao Yang, Qiang Liu, Zhang Li, Zhiyin Ma, Shuo Zhang, and Xiang Bai. 2026. Textmonkey: An ocr-free large multimodal model for understanding document. *IEEE Transactions on Pattern Analysis and Machine Intelligence* (2026).
- [18] Dang Nguyen, Jian Chen, Yu Wang, Gang Wu, Namyong Park, Zhengmian Hu, Hanjia Lyu, Junda Wu, Ryan Aponte, Yu Xia, et al. 2025. Gui agents: A survey. In *Findings of the Association for Computational Linguistics: ACL 2025*. 22522–22538.
- [19] Ajay Patel, Markus Hofmarcher, Claudiu Leoveanu-Condrei, Marius-Constantin Dinu, Chris Callison-Burch, and Sepp Hochreiter. 2024. Large language models can self-improve at web agent tasks. *arXiv preprint arXiv:2405.20309* (2024).
- [20] Pranav Putta, Edmund Mills, Naman Garg, Sumeet Motwani, Chelsea Finn, Divyansh Garg, and Rafael Rafailov. 2024. Agent g: Advanced reasoning and learning for autonomous ai agents. *arXiv preprint arXiv:2408.07199* (2024).
- [21] Zehan Qi, Xiao Liu, Iat Long long, Hanyu Lai, Xueqiao Sun, Wenyi Zhao, Yu Yang, Xinyue Yang, Jiada Sun, Shuntian Yao, et al. 2024. Webrl: Training llm web agents via self-evolving online curriculum reinforcement learning. *arXiv preprint arXiv:2411.02337* (2024).
- [22] Yujia Qin, Yining Ye, Junjie Fang, Haoming Wang, Shihao Liang, Shizuo Tian, Junda Zhang, Jiahao Li, Yunxin Li, Shijue Huang, et al. 2025. Ui-tars: Pioneering automated gui interaction with native agents. *arXiv preprint arXiv:2501.12326* (2025).
- [23] Christopher Rawles, Alice Li, Daniel Rodriguez, Oriana Riva, and Timothy Lilliprap. 2023. Androidinthewild: A large-scale dataset for android device control. *Advances in Neural Information Processing Systems* 36 (2023), 59708–59728.
- [24] Yuzhang Shang, Mu Cai, Bingxin Xu, Yong Jae Lee, and Yan Yan. 2025. Llava-prumerge: Adaptive token reduction for efficient large multimodal models. In *Proceedings of the IEEE/CVF International Conference on Computer Vision*. 22857–22867.
- [25] Rui Shao, Xiangyuan Lan, Jiawei Li, and Pong C Yuen. 2019. Multi-adversarial discriminative deep domain generalization for face presentation attack detection. In *Proceedings of the IEEE/CVF conference on computer vision and pattern recognition*. 10023–10031.
- [26] Rui Shao, Tianxing Wu, and Ziwei Liu. 2023. Detecting and grounding multimodal media manipulation. In *Proceedings of the IEEE/CVF Conference on Computer Vision and Pattern Recognition*. 6904–6913.
- [27] Aleksandar Shtedritski, Christian Rupprecht, and Andrea Vedaldi. 2023. What does clip know about a red circle? visual prompt engineering for vlms. In *Proceedings of the IEEE/CVF International Conference on Computer Vision*. 11987–11997.
- [28] Dezhao Tu, Danylo Vashchilenko, Yuzhe Lu, and Panpan Xu. 2024. VL-cache: Sparsity and modality-aware KV cache compression for vision-language model inference acceleration. *arXiv preprint arXiv:2410.23317* (2024).
- [29] Junyang Wang, Haiyang Xu, Haitao Jia, Xi Zhang, Ming Yan, Weizhou Shen, Ji Zhang, Fei Huang, and Jitao Sang. 2024. Mobile-agent-v2: Mobile device operation assistant with effective navigation via multi-agent collaboration. *Advances in Neural Information Processing Systems* 37 (2024), 2686–2710.
- [30] Peng Wang, Shuai Bai, Sinan Tan, Shijie Wang, Zhihao Fan, Jinze Bai, Keqin Chen, Xuejing Liu, Jialin Wang, Wenbin Ge, et al. 2024. Qwen2-vl: Enhancing vision-language model’s perception of the world at any resolution. *arXiv preprint arXiv:2409.12191* (2024).
- [31] Shuai Wang, Weiwen Liu, Jingxuan Chen, Yuqi Zhou, Weinan Gan, Kingshan Zeng, Yuhao Che, Shuai Yu, Xinlong Hao, Kun Shao, et al. 2024. Gui agents with foundation models: A comprehensive survey. *arXiv preprint arXiv:2411.04890* (2024).
- [32] Xinyuan Wang, Bowen Wang, Dunjie Lu, Junlin Yang, Tianbao Xie, Junli Wang, Jiaqi Deng, Xiaole Guo, Yiheng Xu, Chen Henry Wu, et al. 2025. Opencua: Open foundations for computer-use agents. *arXiv preprint arXiv:2508.09123* (2025).
- [33] Hao Wen, Yuanchun Li, Guohong Liu, Shanhui Zhao, Tao Yu, Toby Jia-Jun Li, Shiqi Jiang, Yunhao Liu, Yaqin Zhang, and Yunxin Liu. 2024. Autodroid: Llm-powered task automation in android. In *Proceedings of the 30th Annual International Conference on Mobile Computing and Networking*. 543–557.

- [34] Zhiyong Wu, Zhenyu Wu, Fangzhi Xu, Yian Wang, Qiushi Sun, Chengyou Jia, Kanzhi Cheng, Zichen Ding, Liheng Chen, Paul Pu Liang, et al. 2024. Os-atlas: A foundation action model for generalist gui agents. *arXiv preprint arXiv:2410.23218* (2024).
- [35] Guangxuan Xiao, Yuandong Tian, Beidi Chen, Song Han, and Mike Lewis. 2023. Efficient streaming language models with attention sinks. *arXiv preprint arXiv:2309.17453* (2023).
- [36] Tianbao Xie, Danyang Zhang, Jixuan Chen, Xiaochuan Li, Siheng Zhao, Ruisheng Cao, Toh J Hua, Zhoujun Cheng, Dongchan Shin, Fangyu Lei, et al. 2024. Os-world: Benchmarking multimodal agents for open-ended tasks in real computer environments. *Advances in Neural Information Processing Systems* 37 (2024), 52040–52094.
- [37] Xubing Ye, Yukang Gan, Xiaoke Huang, Yixiao Ge, and Yansong Tang. 2025. Vocolama: Towards vision compression with large language models. In *Proceedings of the Computer Vision and Pattern Recognition Conference*. 29836–29846.
- [38] Keen You, Haotian Zhang, Eldon Schoop, Floris Weers, Amanda Swearingin, Jeffrey Nichols, Yinfei Yang, and Zhe Gan. 2024. Ferret-ui: Grounded mobile ui understanding with multimodal llms. In *European Conference on Computer Vision*. Springer, 240–255.
- [39] Chi Zhang, Zhao Yang, Jiaxuan Liu, Yanda Li, Yucheng Han, Xin Chen, Zebiao Huang, Bin Fu, and Gang Yu. 2025. Appagent: Multimodal agents as smartphone users. In *Proceedings of the 2025 CHI Conference on Human Factors in Computing Systems*. 1–20.
- [40] Renshan Zhang, Rui Shao, Gongwei Chen, Miao Zhang, Kaiwen Zhou, Weili Guan, and Liqiang Nie. 2025. Falcon: Resolving visual redundancy and fragmentation in high-resolution multimodal large language models via visual registers. In *Proceedings of the IEEE/CVF International Conference on Computer Vision*. 23530–23540.
- [41] Zhenyu Zhang, Ying Sheng, Tianyi Zhou, Tianlong Chen, Lianmin Zheng, Ruisi Cai, Zhao Song, Yuandong Tian, Christopher Ré, Clark Barrett, et al. 2023. H2o: Heavy-hitter oracle for efficient generative inference of large language models. *Advances in Neural Information Processing Systems* 36 (2023), 34661–34710.
- [42] Boyuan Zheng, Boyu Gou, Jihyung Kil, Huan Sun, and Yu Su. 2024. Gpt-4v (ision) is a generalist web agent, if grounded. *arXiv preprint arXiv:2401.01614* (2024).

A GUI Navigation Tasks

ScreenSpot Pro [10]. ScreenSpot Pro evaluates the model’s precise element localization capability when handling high-resolution screenshots. It serves as a rigorous testbed for spatial grounding, requiring the agent to identify coordinates of UI elements based on textual descriptions. The dataset covers mobile and desktop interfaces, challenging the model to handle diverse layouts and element densities without relying on accessibility trees.

ScreenSpotV2 [34]. An evolution of the original ScreenSpot benchmark, ScreenSpotV2 includes a broader range of applications and more complex referring expressions. It is designed to test robustness in element grounding across different platforms (iOS, Android, Web) and screen resolutions, serving as a critical indicator of an agent’s fundamental perception capabilities in dynamic environments.

Android In The Wild (AITW) [23]. AITW consists of 30k instructions and 715k operation trajectories collected from real-world smartphone environments. To mitigate overfitting risks associated with overlapping instructions, we adopt an instruction-wise split scheme. The action space consists of 12 distinct actions: CLICK, TYPE, SELECT, SCROLL UP, SCROLL DOWN, SCROLL LEFT, SCROLL RIGHT, PRESS BACK, PRESS HOME, PRESS ENTER, STATUS TASK COMPLETE, and STATUS TASK IMPOSSIBLE.

Multimodal-Mind2Web [42]. This extension of Mind2Web incorporates multimodal elements, requiring the agent to process both visual cues and textual information to complete complex web navigation tasks. Unlike the text-only version, it tests the agent’s ability to integrate cross-modal information for decision-making in rich web environments where visual layout plays a crucial role in understanding context.

AndroidControl [11]. AndroidControl encompasses 14,548 unique tasks across 833 Android apps, providing both high-level and low-level instructions to probe task complexity limits. We adhere to standard evaluation settings. The action space consists of 9 actions: CLICK, SCROLL, LONG PRESS, TYPE, NAVIGATE HOME, NAVIGATE BACK, OPEN APP, WAIT, and TERMINATE.

AgentNetBench [32]. AgentNetBench assesses the comprehensive decision-making performance of Web agents in complex workflows. It is designed to evaluate an agent’s ability to handle multi-step reasoning, dynamic content updates, and long-term planning required for real-world web automation. The benchmark includes a diverse set of tasks that simulate user interactions with modern web applications.

OSWorld-Verified [36]. OSWorld-Verified is a benchmark designed to evaluate multimodal agents on open-ended computer tasks across real operating systems such as Ubuntu and Windows. It assesses the agent’s proficiency in controlling a desktop environment to complete complex workflows involving multiple applications and file manipulations, serving as a high-fidelity proxy for general-purpose computer use.

B Implementation Details

To ensure a comprehensive evaluation, we instantiate our framework on two state-of-the-art GUI agent backbones: **UI-TARS-1.5-7B [22]** and **OpenCUA-7B [32]**.

UI-TARS-1.5-7B. UI-TARS is a specialized Vision-Language Model (VLM) based on the Qwen2.5-VL [1] architecture, fine-tuned specifically for GUI interaction tasks. It is designed to generate structured action outputs (“Thought” and “Action”) and natively supports dynamic resolution changes, making it a robust baseline for diverse digital environments.

OpenCUA. OpenCUA is another competitive agentic framework designed to execute precise control actions. Built upon the Qwen2-VL [30] architecture, it utilizes a specific system prompt tailored for pyautogui execution, emphasizing the generation of executable Python-like commands for controlling the interface via a standard API.

B.1 Prompt Templates

We adopt the official inference prompts for both models as defined in their respective codebases to ensure fair comparison.

UI-TARS Inference Prompt

You are a GUI agent. Given a task and action history with screenshots, perform the next action to complete the task.

Output Format

Thought: [Reasoning Plan]
Action: [Function Call]

Action Space

click(point) long_press(point)
type(content) open_app(app_name)
scroll(point, direction) drag(start_point, end_point)
press_home() press_back() finished(content)

User Instruction

{instruction}

OpenCUA Prompt Configuration. For OpenCUA, the prompt structure includes a specialized system message defining the agent’s

role in executing pyautogui actions. The history is provided as a sequence of image-text pairs.

OpenCUA Inference Prompt

You are a GUI agent. Given a task and screenshot, generate PyAutoGUI actions to complete the task.

Output Format

Thought: [Progress Assessment & Recovery Strategy]
Action: [PyAutoGUI Code or Function Call]

Action Space

Standard PyAutoGUI Commands (click, type, hotkey...)
computer.triple_click(x, y)
computer.terminate(status='success'|'failure')

User Instruction
{instruction}

B.2 Model Configurations

Resolution Settings: We strictly adhere to the native resolution constraints of the base models. Specifically, for the Qwen2.5-VL backbone used in UI-TARS, we utilize the AutoProcessor with dynamic resolution support. The input images are processed with `min_pixels` set to $256 \times 28 \times 28$ and `max_pixels` set to $16384 \times 28 \times 28$.

Acceleration: To optimize inference efficiency, all models are loaded with `bf16` precision. We leverage **Flash Attention 2** for accelerated attention computation, which is critical for handling the long sequences generated by multi-turn GUI interactions.

C Algorithm Details

Algorithm 1 formalizes the execution flow of the ST-Lite framework. Given the full KV cache from the prefill phase, the procedure compresses it to a target budget B based on the integrated spatio-trajectory scores.

D Full Experimental Results

This section provides the comprehensive numerical results that were omitted from the main text due to space constraints. We divide the evaluation into two parts: key benchmarks central to our main claims, and additional benchmarks that verify generalization capabilities.

D.1 Performance on Key Benchmarks

Detailed performance comparisons on ScreenSpot Pro, AITW, and AgentNetBench across different budget ratios are presented in Table 4 at the end of this appendix. As observed, our method maintains high performance even at low budgets.

D.2 Performance on Additional Benchmarks

To verify the robustness of our method across diverse mobile and web platforms, we extended the evaluation to **ScreenSpotV2**, **AndroidControl**, **Multimodal-Mind2Web**, and **OSWorld-Verified**. These results are summarized in Table 5. It is worth noting that even in tasks involving complex Android control commands or multi-step web interactions, ST-Lite maintains a stable performance advantage.

Algorithm 1 ST-Lite Compression Procedure

Require: $\mathbf{K}, \mathbf{V} \in \mathbb{R}^{L \times D}$: Full Key-Value Cache

\mathbf{Q}_{cur} : Current Query States

$\beta \in (0, 1]$: Target Budget Ratio

δ : Observation Window Size

Ensure: \mathbf{K}', \mathbf{V}' : Compressed Cache

- 1: **Initialization:**
- 2: $B \leftarrow \lfloor \beta \cdot L \rfloor$
- 3: $\mathbf{S} \leftarrow \mathbf{0}^L$ {Initialize score vector}
- 4: **Procedure ComputeScores**($\mathbf{K}, \mathbf{Q}_{cur}$):
- 5: **for** $i \in \{1, \dots, L\}$ **do**
- 6: $A_{base}^{(i)} \leftarrow \sum_{q \in \text{Window}(\delta)} \text{Softmax}(\frac{q \cdot \mathbf{k}_i^T}{\sqrt{d}})$
- 7: **if** i is Visual Token at (u, v) **then**
- 8: $\mathcal{H}_{u,v} \leftarrow \frac{1}{|N_{u,v}|} \sum_{j \in N_{u,v}} \frac{\mathbf{k}_i \cdot \mathbf{k}_j}{\|\mathbf{k}_i\| \|\mathbf{k}_j\|}$ {Eq. 7}
- 9: $\Phi_{space}^{(i)} \leftarrow 1 - \mathcal{H}_{u,v}$
- 10: $\rho_i \leftarrow \max_{h \in \mathbf{Q}_{cur}} \text{CosSim}(\mathbf{k}_i, h)$
- 11: $\mathcal{T}_{pool} \leftarrow \mathcal{T}_{pool} \cup \{\rho_i\}$
- 12: **end if**
- 13: **end for**
- 14: **Procedure Thresholding**(\mathcal{T}_{pool}, B):
- 15: $\hat{\rho} \leftarrow \text{Sort}_{\text{asc}}(\mathcal{T}_{pool})$
- 16: $\tau_{red} \leftarrow \hat{\rho}[B]$ {Eq. 10}
- 17: **Procedure Integration & Eviction:**
- 18: **for** $i \in \{1, \dots, L\}$ **do**
- 19: **if** i is Visual Token **then**
- 20: $M_{time}^{(i)} \leftarrow \mathbb{I}(\rho_i \leq \tau_{red})$ {Eq. 11}
- 21: $\mathbf{S}^{(i)} \leftarrow M_{time}^{(i)} \cdot (A_{base}^{(i)} + \Phi_{space}^{(i)})$
- 22: **else**
- 23: $\mathbf{S}^{(i)} \leftarrow A_{base}^{(i)}$
- 24: **end if**
- 25: **end for**
- 26: $\mathcal{I}_{keep} \leftarrow \text{TopK}(\mathbf{S}, B)$
- 27: **return** $\mathbf{K}[\mathcal{I}_{keep}], \mathbf{V}[\mathcal{I}_{keep}]$

E Detailed Latency Analysis

Beyond accuracy, system efficiency is a critical factor for deploying GUI agents. Table 3 breaks down the latency metrics (Prefill vs. Decoding) for varying trajectory lengths. ST-Lite significantly reduces decoding latency by compressing the KV cache, which directly translates to a **1.4** \times end-to-end speedup. Note that prefill latency remains comparable as our compression takes effect post-prefill.

Table 3: Detailed Latency and Speedup Analysis.

Screenshots	Prefill Latency (ms)		Decoding Latency (ms)		Speedup		
	Full Cache	ST-Lite	Full Cache	ST-Lite	Prefill	Decoding	End-to-End
3	1656.4	1690.2	3888.8	3111.4	0.98	1.25	1.15
5	2516.4	2541.8	4063.8	2402.9	0.99	1.68	1.33
10	4685.3	4732.6	4501.1	1837.2	0.99	2.45	1.4

F Extended Qualitative Analysis

Figure 8 visualizes the token retention patterns on a multi-step flight search task (Mexico City to Zurich) under a 20% cache budget. As observed, **SnapKV** (Row 1) completely discards early historical

frames, losing critical context like the origin city input. **PyramidKV** and **VL-Cache** (Rows 2-3) exhibit fragmented retention, resulting in a “mosaic” effect that breaks the semantic integrity of text and buttons. In contrast, **ST-Lite** (Row 4) successfully preserves the complete structure of interactive elements and essential historical inputs while filtering out static background noise.

G Limitations

While our framework achieves significant efficiency gains by leveraging structural and historical priors, there remains potential to further align the compression strategy with the model’s internal representation dynamics through data-driven optimization. Future work will explore end-to-end learnable policies to facilitate the deployment of Large Vision-Language Models in even more complex scenarios. Moreover, we aim to synergize this compression philosophy with advanced agentic training paradigms (e.g., Reinforcement Learning), fostering a unified framework where efficient memory mechanisms and decision-making policies are co-optimized.

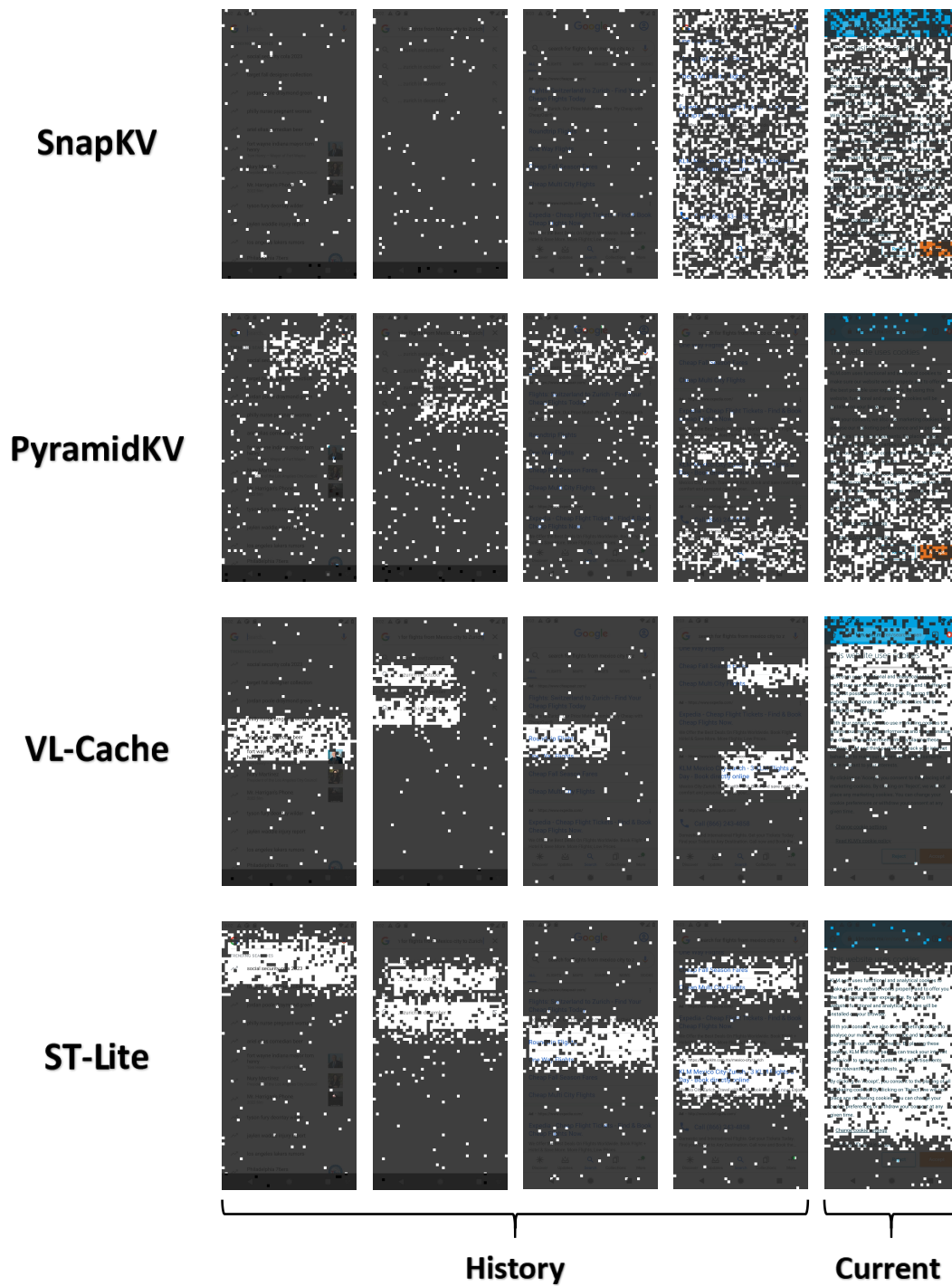


Figure 8: Visualization of token retention patterns on a 5-step trajectory for the task “Search for flights from Mexico City to Zurich”. The figure displays the retained visual tokens (highlighted regions) versus evicted ones (dark regions) for SnapKV, PyramidKV, VL-Cache, and ST-Lite across historical and current frames.

Table 4: Detailed performance comparison on key benchmarks (ScreenSpot Pro, AITW, and AgentNetBench) across different budget ratios.

Dataset	Model	Method	Budget								Δ	
			1%	3%	5%	10%	15%	20%	40%	80%		100%
ScreenSpot Pro	UI-TARS-1.5-7B	SnapKV	6.9	23.6	29.3	36.8	38.6	39.7	40.1	42.1	42.3	
		PyramidKV	4.8	14.1	20.9	26.5	29.9	34.6	38.9	41.3	42.3	
		VL-Cache	1.1	15.8	23.9	32.2	34.6	36.7	40.3	41.4	42.3	
		ST-Lite (CSS only)	7.3	23.4	31.0	36.9	39.1	42.2	42.7	43.4	42.3	
		ST-Lite	7.3	23.4	31.0	36.9	39.1	42.2	42.7	43.4	42.3	+1.1
	OpenCUA-7B	SnapKV	10.0	16.1	18.5	17.7	15.2	17.2	14.7	26.9	43.3	
		PyramidKV	14.9	14.5	14.3	11.9	14.3	12.9	13.9	14.4	43.3	
		VL-Cache	1.1	14.6	15.2	15.6	13.8	16.7	15.1	14.5	43.3	
		ST-Lite (CSS only)	9.5	18.9	20.1	17.9	16.8	19.4	19.3	29.3	43.3	
		ST-Lite	9.5	18.9	20.1	17.9	16.8	19.4	19.3	29.3	43.3	+1.2
AITW	UI-TARS-1.5-7B	SnapKV	8.1	11.5	13.2	14.2	14.5	15.3	15.6	16.6	18.2	
		PyramidKV	8.6	7.5	10.8	14.2	15.1	14.4	15.1	17.2	18.2	
		VL-Cache	0.2	1.7	2.1	9.8	10.5	11.1	10.1	9.1	18.2	
		ST-Lite (CSS only)	8.3	12.4	14.1	15.7	16.7	17.4	16.9	16.7	18.2	
		ST-Lite	8.6	13.2	16.0	18.4	20.0	20.1	19.0	17.1	18.2	+2.7
	OpenCUA-7B	SnapKV	1.6	8.2	11.7	12.5	14.3	14.2	13.1	10.7	17.3	
		PyramidKV	1.3	4.2	8.9	11.7	13.3	12.8	10.9	9.8	17.3	
		VL-Cache	0.0	0.0	0.1	0.6	1.1	2.1	6.7	7.7	17.3	
		ST-Lite (CSS only)	1.9	7.7	11.4	12.2	14.7	14.2	12.9	11.2	17.3	
		ST-Lite	1.5	6.7	10.6	13.3	15.8	16.4	14.3	12.3	17.3	+0.6
AgentNetBench	UI-TARS-1.5-7B	SnapKV	0.4	0.8	1.5	4.1	8.4	9.3	17.8	18.9	17.5	
		PyramidKV	1.4	1.8	0.8	1.3	2.7	4.1	11.0	19.0	17.5	
		VL-Cache	0.0	0.7	1.9	9.8	15.9	16.1	16.9	18.7	17.5	
		ST-Lite (CSS only)	0.9	2.1	2.7	7.7	9.9	14.1	18.1	18.7	17.5	
		ST-Lite	0.1	1.7	3.0	9.8	13.2	17.0	20.7	20.5	17.5	+0.3
	OpenCUA-7B	SnapKV	0.8	3.2	3.7	5.6	6.6	8.0	17.1	28.3	66.4	
		PyramidKV	0.6	0.6	0.8	1.6	2.6	4.7	11.1	26.9	66.4	
		VL-Cache	0.5	2.8	1.9	0.9	4.7	8.1	0.9	19.9	66.4	
		ST-Lite (CSS only)	1.6	1.8	2.3	3.5	6.7	8.4	19.1	28.1	66.4	
		ST-Lite	0.2	6.6	8.7	13.6	15.6	20.8	28.6	37.6	66.4	+7.3

Table 5: Performance evaluation on additional benchmarks (ScreenSpotV2, AndroidControl, Multimodal-Mind2Web, and OSWorld-Verified).

Dataset	Model	Method	Budget								Δ	
			1%	3%	5%	10%	15%	20%	40%	80%		100%
ScreenSpotV2	UI-TARS-1.5-7B	SnapKV	16.1	62.9	77.5	85.2	86.5	88.3	88.2	88.4	88.9	
		PyramidKV	17.0	47.1	55.5	75.5	82.9	84.6	87.5	88.6	88.9	
		VL-Cache	0.0	30.7	53.2	70.8	83.2	85.6	88.0	88.4	88.9	
		ST-Lite (CSS only)	17.1	62.9	79.6	86.0	87.0	88.8	88.4	89.3	88.9	
		ST-Lite	17.1	62.9	79.6	86.0	87.0	88.8	88.4	89.3	88.9	+0.6
	OpenCUA-7B	SnapKV	42.1	71.5	73.8	70.8	64.0	66.3	60.2	74.3	90.7	
		PyramidKV	16.9	34.9	41.7	41.0	41.4	63.3	57.9	74.4	90.7	
		VL-Cache	0.9	52.3	59.0	67.5	57.8	61.1	55.8	74.0	90.7	
		ST-Lite (CSS only)	41.9	71.7	69.9	71.1	65.5	70.4	67.2	77.0	90.7	
		ST-Lite	41.9	71.7	69.9	71.1	65.5	70.4	67.2	77.0	90.7	+1.5
AndroidControl	UI-TARS-1.5-7B	SnapKV	18.9	26.1	28.9	39.1	41.7	44.4	47.7	46.6	49.6	
		PyramidKV	11.6	20.8	24.9	28.9	34.4	37.9	44.6	46.3	49.6	
		VL-Cache	1.9	6.6	10.6	34.9	39.9	42.9	46.3	45.8	49.6	
		ST-Lite (CSS only)	15.9	26.0	30.1	39.7	42.0	43.6	48.7	47.1	49.6	
		ST-Lite	13.9	25.9	34.8	44.2	46.9	48.9	50.3	48.1	49.6	+2.4
	OpenCUA-7B	SnapKV	3.6	15.3	18.6	21.6	27.9	25.9	30.9	26.1	40.7	
		PyramidKV	1.9	15.9	15.9	22.9	27.3	27.9	23.1	26.9	40.7	
		VL-Cache	0.0	2.9	2.5	11.9	15.7	19.5	27.9	6.5	40.7	
		ST-Lite (CSS only)	2.3	14.2	18.8	23.3	29.8	28.7	34.4	29.1	40.7	
		ST-Lite	0.7	15.9	19.9	26.8	36.9	32.9	37.9	34.1	40.7	+3.8
Multimodal-Mind2Web	UI-TARS-1.5-7B	SnapKV	2.1	4.7	7.1	11.6	16.9	18.6	22.7	24.2	25.9	
		PyramidKV	1.4	3.9	4.7	5.9	9.1	11.9	21.9	24.2	25.9	
		VL-Cache	0.0	0.1	0.0	0.6	3.9	7.4	19.9	23.9	25.9	
		ST-Lite (CSS only)	2.4	7.3	10.9	16.4	19.4	20.7	21.9	25.9	25.9	
		ST-Lite	1.9	7.1	12.9	21.4	25.7	27.2	30.2	31.1	25.9	+6.2
	OpenCUA-7B	SnapKV	0.9	2.4	5.6	9.4	12.7	14.3	16.7	17.3	33.6	
		PyramidKV	0.0	0.9	1.8	5.6	6.7	10.9	12.7	14.1	33.6	
		VL-Cache	0.0	0.0	0.0	0.1	0.1	0.0	13.4	14.4	33.6	
		ST-Lite (CSS only)	0.8	0.0	5.7	10.1	11.7	14.4	17.1	1.6	33.6	
		ST-Lite	0.2	1.8	7.8	13.4	15.2	16.9	18.3	19.4	33.6	+1.7
OSWorld-Verified	UI-TARS-1.5-7B	SnapKV	2.2	3.2	6.9	16.6	16.7	18.6	19.2	23.2	26.3	
		PyramidKV	0.2	1.9	1.1	2.9	9.9	15.6	16.9	20.3	26.3	
		VL-Cache	0.0	1.9	10.6	7.6	8.9	9.7	10.1	19.9	26.3	
		ST-Lite (CSS only)	1.9	3.0	7.1	17.3	18.2	19.6	23.1	25.3	26.3	
		ST-Lite	0.6	1.1	8.6	18.9	19.7	25.9	27.0	28.1	26.3	+2.4
	OpenCUA-7B	SnapKV	0.7	0.9	0.5	6.9	10.1	14.3	16.2	16.8	23.8	
		PyramidKV	0.3	0.9	1.9	6.7	8.6	11.2	13.1	14.9	23.8	
		VL-Cache	0.0	0.1	0.6	3.1	6.9	9.9	9.7	9.1	23.8	
		ST-Lite (CSS only)	1.1	1.4	3.3	6.9	10.9	14.7	17.4	17.9	23.8	
		ST-Lite	0.1	0.9	4.1	8.9	13.9	16.9	19.7	17.5	23.8	+1.8